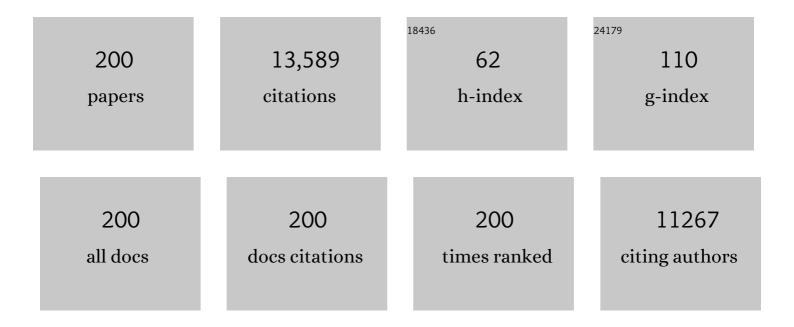
## Kenneth S Vecchio

List of Publications by Year in descending order

Source: https://exaly.com/author-pdf/7284832/publications.pdf Version: 2024-02-01



#	Article	IF	CITATIONS
1	Color and pseudogap tunability in multicomponent carbonitrides. Materials and Design, 2022, 217, 110600.	3.3	2
2	Processing-dependent stabilization of a dissimilar rare-earth boride in high-entropy (Ti0.2Zr0.2Hf0.2Ta0.2Er0.2)B2 with enhanced hardness and grain boundary segregation. Journal of the European Ceramic Society, 2022, 42, 5164-5171.	2.8	11
3	Efficient few-shot machine learning for classification of EBSD patterns. Scientific Reports, 2021, 11, 8172.	1.6	17
4	High-entropy rare earth tetraborides. Journal of the European Ceramic Society, 2021, 41, 2968-2973.	2.8	28
5	An Acquisition Parameter Study for Machine-Learning-Enabled Electron Backscatter Diffraction. Microscopy and Microanalysis, 2021, 27, 776-793.	0.2	4
6	Autonomous EBSD Pattern Classification Performance with Changing Acquisition Parameters. Microscopy and Microanalysis, 2021, 27, 2490-2493.	0.2	0
7	Mesoscale hetero-deformation induced (HDI) stress in FeAl-based metallic-intermetallic laminate (MIL) composites. Acta Materialia, 2021, 213, 116949.	3.8	13
8	A universal configurational entropy metric for high-entropy materials. Scripta Materialia, 2021, 201, 113974.	2.6	64
9	Bulk high-entropy hexaborides. Journal of the European Ceramic Society, 2021, 41, 5775-5781.	2.8	22
10	High-throughput rapid experimental alloy development (HT-READ). Acta Materialia, 2021, 221, 117352.	3.8	23
11	Development of ultrahigh-entropy ceramics with tailored oxidation behavior. Journal of the European Ceramic Society, 2021, 41, 5791-5800.	2.8	29
12	Enhancing plasticity in high-entropy refractory ceramics via tailoring valence electron concentration. Materials and Design, 2021, 209, 109932.	3.3	32
13	Orientation-dependent superelasticity of a metastable high-entropy alloy. Applied Physics Letters, 2021, 119, 161908.	1.5	3
14	Novel remapping approach for HR-EBSD based on demons registration. Ultramicroscopy, 2020, 208, 112851.	0.8	20
15	A computer vision approach to study surface deformation of materials. Measurement Science and Technology, 2020, 31, 055602.	1.4	10
16	Thermal conductivity and hardness of three single-phase high-entropy metal diborides fabricated by borocarbothermal reduction and spark plasma sintering. Ceramics International, 2020, 46, 6906-6913.	2.3	107
17	High-entropy monoborides: Towards superhard materials. Scripta Materialia, 2020, 189, 101-105.	2.6	57
18	The effect of oxides on Fe/Al interfacial reaction in Metal-Intermetallic Laminate (MIL) composites. Journal of Alloys and Compounds, 2020, 845, 156268.	2.8	10

#	Article	IF	CITATIONS
19	Cold-workable refractory complex concentrated alloys with tunable microstructure and good room-temperature tensile behavior. Scripta Materialia, 2020, 188, 16-20.	2.6	24
20	Searching for high entropy alloys: A machine learning approach. Acta Materialia, 2020, 198, 178-222.	3.8	107
21	Bulk high-entropy nitrides and carbonitrides. Scientific Reports, 2020, 10, 21288.	1.6	85
22	Design, fabrication and optimization of FeAl–FeAl2 eutectoid metallic-intermetallic laminate (MIL) composites. Materialia, 2020, 13, 100859.	1.3	9
23	Phase Mapping in EBSD Using Convolutional Neural Networks. Microscopy and Microanalysis, 2020, 26, 458-468.	0.2	17
24	Deep Neural Network Enabled Space Group Identification in EBSD. Microscopy and Microanalysis, 2020, 26, 447-457.	0.2	21
25	Electromigration effect in Fe-Al diffusion couples with field-assisted sintering. Acta Materialia, 2020, 186, 631-643.	3.8	32
26	Crystal symmetry determination in electron diffraction using machine learning. Science, 2020, 367, 564-568.	6.0	99
27	Discovery of high-entropy ceramics via machine learning. Npj Computational Materials, 2020, 6, .	3.5	133
28	Deformation and fracture evolution of FeAl-based metallic-intermetallic laminate (MIL) composites. Acta Materialia, 2020, 194, 496-515.	3.8	20
29	Aged metastable high-entropy alloys with heterogeneous lamella structure for superior strength-ductility synergy. Acta Materialia, 2020, 199, 602-612.	3.8	72
30	Dissolving and stabilizing soft WB2 and MoB2 phases into high-entropy borides via boron-metals reactive sintering to attain higher hardness. Journal of the European Ceramic Society, 2020, 40, 4348-4353.	2.8	71
31	Dual-phase high-entropy ultra-high temperature ceramics. Journal of the European Ceramic Society, 2020, 40, 5037-5050.	2.8	91
32	Spark plasma sintering of structureâ€ŧailored ultrahighâ€ŧemperature components: First step to complex netÂshaping. Journal of the American Ceramic Society, 2019, 102, 548-558.	1.9	9
33	Extraordinary strength-ductility synergy in a heterogeneous-structured $\hat{I}^2$ -Ti alloy through microstructural optimization. Materials Research Letters, 2019, 7, 467-473.	4.1	61
34	Automated Reconstruction of Spherical Kikuchi Maps. Microscopy and Microanalysis, 2019, 25, 912-923.	0.2	9
35	Effect of twinned-structure on deformation behavior and correlated mechanical properties in a metastable Î <sup>2</sup> -Ti alloy. Journal of Alloys and Compounds, 2019, 811, 152054.	2.8	6
36	High-Throughput Identification of Crystal Structures Via Machine Learning. Microscopy and Microanalysis, 2019, 25, 2258-2259.	0.2	0

#	Article	IF	CITATIONS
37	Design, fabrication and characterization of FeAl-based metallic-intermetallic laminate (MIL) composites. Acta Materialia, 2019, 175, 445-456.	3.8	36
38	Reactive flash spark plasma sintering of high-entropy ultrahigh temperature ceramics. Scripta Materialia, 2019, 170, 106-110.	2.6	101
39	A high-entropy silicide: (Mo0.2Nb0.2Ta0.2Ti0.2W0.2)Si2. Journal of Materiomics, 2019, 5, 337-343.	2.8	159
40	Phase stability and mechanical properties of novel high entropy transition metal carbides. Acta Materialia, 2019, 166, 271-280.	3.8	422
41	Grain boundary precipitation of tantalum and NiAl in superelastic FeNiCoAlTaB alloy. Materials Science & Engineering A: Structural Materials: Properties, Microstructure and Processing, 2019, 743, 372-381.	2.6	29
42	Non-equiatomic FeNiCoAl-based high entropy alloys with multiscale heterogeneous lamella structure for strength and ductility. Materials Science & Engineering A: Structural Materials: Properties, Microstructure and Processing, 2019, 743, 361-371.	2.6	50
43	Multifunctional Nonâ€Equiatomic High Entropy Alloys with Superelastic, High Damping, and Excellent Cryogenic Properties. Advanced Engineering Materials, 2019, 21, 1800941.	1.6	31
44	High-entropy fluorite oxides. Journal of the European Ceramic Society, 2018, 38, 3578-3584.	2.8	399
45	Spark erosion as a high-throughput method for producing bimodal nanostructured 316L stainless steel powder. Powder Technology, 2018, 328, 156-166.	2.1	11
46	Application of a novel new multispectral nanoparticle tracking technique. Measurement Science and Technology, 2018, 29, 065002.	1.4	10
47	Observations on {332}<113> twinning-induced softening in Ti-Nb Gum metal. Materials Science & Engineering A: Structural Materials: Properties, Microstructure and Processing, 2018, 724, 189-198.	2.6	21
48	A new class of high-entropy perovskite oxides. Scripta Materialia, 2018, 142, 116-120.	2.6	560
49	High-entropy high-hardness metal carbides discovered by entropy descriptors. Nature Communications, 2018, 9, 4980.	5.8	604
50	Dislocation-type evolution in quasi-statically compressed polycrystalline nickel. Acta Materialia, 2018, 155, 104-116.	3.8	124
51	Design of non-equiatomic high entropy alloys with heterogeneous lamella structure towards strength-ductility synergy. Scripta Materialia, 2018, 154, 78-82.	2.6	67
52	The search for high entropy alloys: A high-throughput ab-initio approach. Acta Materialia, 2018, 159, 364-383.	3.8	142
53	Enhancement of <001> recrystallization texture in non-equiatomic Fe-Ni-Co-Al-based high entropy alloys by combination of annealing and Cr addition. Journal of Alloys and Compounds, 2018, 768, 277-286.	2.8	18
54	Lightweight Open-Cell Scaffolds from Sea Urchin Spines with Superior Material Properties for Bone Defect Repair. ACS Applied Materials & Interfaces, 2017, 9, 9862-9870.	4.0	15

#	Article	IF	CITATIONS
55	An experimental investigation on the notch toughness of Cu-Zr-based bulk metallic glasses with in-situ crystallization. Journal of Non-Crystalline Solids, 2017, 469, 70-78.	1.5	14
56	Microstructure evolution in Ni and Ni-superalloy based metallic-intermetallic laminate (MIL) composites. Intermetallics, 2017, 87, 70-80.	1.8	18
57	Investigation of the shear response and geometrically necessary dislocation densities in shear localization in high-purity titanium. International Journal of Plasticity, 2017, 92, 148-163.	4.1	31
58	Dynamic deformation and failure of ultrafine-grained titanium. Acta Materialia, 2017, 125, 210-218.	3.8	82
59	Phase stability dependence of deformation mode correlated mechanical properties and elastic properties in Ti-Nb gum metal. Materials Science & Engineering A: Structural Materials: Properties, Microstructure and Processing, 2017, 702, 173-183.	2.6	19
60	Dynamic compressive strength and mechanism of failure of Al-W fiber composite tubes with ordered mesostructure. International Journal of Impact Engineering, 2017, 100, 1-6.	2.4	8
61	Optimizing Bulk Metallic Glasses for Robust, Highly Wearâ€Resistant Gears. Advanced Engineering Materials, 2017, 19, 1600541.	1.6	54
62	Microstructure evolution in pure Ni and Invar-based Metallic-Intermetallic Laminate (MIL) composites. Materials Science & Engineering A: Structural Materials: Properties, Microstructure and Processing, 2017, 682, 454-465.	2.6	19
63	Effects of aging and cooling rate on the transformation of nanostructured Ti-50.8Ni. Journal of Alloys and Compounds, 2017, 693, 150-163.	2.8	11
64	High-Entropy Metal Diborides: A New Class of High-Entropy Materials and a New Type of Ultrahigh Temperature Ceramics. Scientific Reports, 2016, 6, 37946.	1.6	721
65	Effect of zirconium purity on the glass-forming-ability and notch toughness of Cu43Zr43Al7Be7. Materials Science & Engineering A: Structural Materials: Properties, Microstructure and Processing, 2016, 674, 397-405.	2.6	3
66	Determination of geometrically necessary dislocations in large shear strain localization in aluminum. Acta Materialia, 2016, 118, 383-394.	3.8	76
67	Fragmentation and constitutive response of tailored mesostructured aluminum compacts. Journal of Applied Physics, 2016, 119, .	1.1	11
68	Annealing effects on the microstructure and properties of an Fe-based Metallic-Intermetallic Laminate (MIL) composite. Materials Science & Engineering A: Structural Materials: Properties, Microstructure and Processing, 2016, 665, 47-58.	2.6	21
69	Microstructure evolution in Fe-based-aluminide metallic–intermetallic laminate (MIL) composites. Materials Science & Engineering A: Structural Materials: Properties, Microstructure and Processing, 2016, 649, 325-337.	2.6	52
70	Fracture toughness of Ceramic-Fiber-Reinforced Metallic-Intermetallic-Laminate (CFR-MIL) composites. Materials Science & Engineering A: Structural Materials: Properties, Microstructure and Processing, 2016, 649, 407-416.	2.6	68
71	Microstructure evolution in a martensitic 430 stainless steel–Al metallic–intermetallic laminate (MIL) composite. Materials Science & Engineering A: Structural Materials: Properties, Microstructure and Processing, 2015, 643, 72-85.	2.6	39
72	Investigation into dynamic response of a three-point bend specimen in a Hopkinson bar loaded fracture test using numerical methods. Advances in Mechanical Engineering, 2015, 7, 168781401559131.	0.8	1

#	Article	IF	CITATIONS
73	Numerical Investigation of the Ballistic Performance of Metal-Intermetallic Laminate Composites. Applied Composite Materials, 2015, 22, 437-456.	1.3	29
74	Calcium phosphate-bearing matrices induce osteogenic differentiation of stem cells through adenosine signaling. Proceedings of the National Academy of Sciences of the United States of America, 2014, 111, 990-995.	3.3	302
75	Catalytic Effect of Ni and Fe Addition to Gasifier Bed Material in the Steam Reforming of Producer Gas. Industrial & Engineering Chemistry Research, 2014, 53, 13656-13666.	1.8	32
76	Conversion of natural marine skeletons as scaffolds for bone tissue engineering. Frontiers of Materials Science, 2013, 7, 103-117.	1.1	54
77	Tar and CO2 removal from simulated producer gas with activated carbon and charcoal. Fuel Processing Technology, 2013, 106, 201-208.	3.7	26
78	Three-dimensional scaffolding to investigate neuronal derivatives of human embryonic stem cells. Biomedical Microdevices, 2012, 14, 829-838.	1.4	60
79	Cancer cell migration within 3D layer-by-layer microfabricated photocrosslinked PEG scaffolds with tunable stiffness. Biomaterials, 2012, 33, 7064-7070.	5.7	107
80	Wallner lines in a nanocrystalline Ni–23% Fe alloy. Scripta Materialia, 2012, 67, 907-910.	2.6	1
81	Bacterial Toxin-Triggered Drug Release from Gold Nanoparticle-Stabilized Liposomes for the Treatment of Bacterial Infection. Journal of the American Chemical Society, 2011, 133, 4132-4139.	6.6	243
82	Evolution of Iridium-Based Molecular Catalysts during Water Oxidation with Ceric Ammonium Nitrate. Journal of the American Chemical Society, 2011, 133, 19024-19027.	6.6	193
83	Thermal stability and crystallization phenomena of low cost Ti-based bulk metallic glass. Journal of Non-Crystalline Solids, 2011, 357, 3393-3398.	1.5	15
84	Loading rate effects on the R-curve behavior of cortical bone. Acta Biomaterialia, 2011, 7, 724-732.	4.1	45
85	Effects of ductile phase volume fraction on the mechanical properties of Ti–Al3Ti metal-intermetallic laminate (MIL) composites. Materials Science & Engineering A: Structural Materials: Properties, Microstructure and Processing, 2011, 528, 3134-3146.	2.6	120
86	Effects of age and loading rate on equine cortical bone failure. Journal of the Mechanical Behavior of Biomedical Materials, 2011, 4, 57-75.	1.5	76
87	A study of the dynamic compressive behavior of Elk antler. Materials Science and Engineering C, 2011, 31, 1030-1041.	3.8	17
88	Aging effects on hardness and dynamic compressive behavior of Ti–55Ni (at.%) alloy. Materials Science & Engineering A: Structural Materials: Properties, Microstructure and Processing, 2010, 527, 1665-1676.	2.6	63
89	Influence of cold work and texture on the high-strain-rate response of Nitinol. Materials Science & Engineering A: Structural Materials: Properties, Microstructure and Processing, 2010, 527, 5255-5267.	2.6	13
90	Use of Brazilian disk test to determine properties of metallic-intermetallic laminate composites. Jom, 2010, 62, 35-40.	0.9	26

#	Article	IF	CITATIONS
91	Dynamic fracture resilience of elk antler: Biomimetic inspiration for improved crashworthiness. Jom, 2010, 62, 41-46.	0.9	9
92	Influence of anisotropy (crystallographic and microstructural) on spallation in Zr, Ta, HY-100 steel, and 1080 eutectoid steel. International Journal of Fracture, 2010, 163, 243-258.	1.1	29
93	Templated Mineralization of Synthetic Hydrogels for Bone-Like Composite Materials: Role of Matrix Hydrophobicity. Biomacromolecules, 2010, 11, 2060-2068.	2.6	69
94	Stimuli-Responsive Liposome Fusion Mediated by Gold Nanoparticles. ACS Nano, 2010, 4, 1935-1942.	7.3	145
95	Aspectos microestruturais da falha de um aço IF deformado via compressão dinâmica a -196ºC. Revista Escola De Minas, 2009, 62, 167-173.	0.1	1
96	The response of carbon nanotube ensembles to fluid flow: Applications to mechanical property measurement and diagnostics. Journal of Applied Physics, 2009, 106, .	1.1	15
97	High Strength (Ti <sub>58</sub> Ni <sub>28</sub> Cu <sub>8</sub> Si <sub>4</sub> Sn <sub>2</sub> ) <sub>100â°'<i>x</i></sub> Nanoeutectic Matrix– <i>β</i> â€Ti Dendrite, BMGâ€Derived Composites with Enhanced Plasticity and Corrosion Resistance, Advanced Engineering Materials, 2009, 11, 885-891.	b>Mo <sul 1.6</sul 	o>≺i>x
98	Semi-solid induction forging of metallic glass matrix composites. Jom, 2009, 61, 11-17.	0.9	40
99	Mechanical Behavior and Microstructural Development of Low-Carbon Steel and Microcomposite Steel Reinforcement Bars Deformed under Quasi-Static and Dynamic Shear Loading. Metallurgical and Materials Transactions A: Physical Metallurgy and Materials Science, 2009, 40, 1835-1850.	1.1	21
100	Modeling the amorphous forming ability of Ti-based alloys with wide supercooled liquid regions and high hardness. Materials Science & Engineering A: Structural Materials: Properties, Microstructure and Processing, 2009, 506, 94-100.	2.6	20
101	Development of bioresorbable Mg-substituted tricalcium phosphate scaffolds for bone tissue engineering. Materials Science and Engineering C, 2009, 29, 2003-2010.	3.8	11
102	Dimensional control of multi-walled carbon nanotubes in floating-catalyst CVD synthesis. Carbon, 2009, 47, 2085-2094.	5.4	54
103	Evaluation of glass-forming ability in metals using multi-model techniques. Journal of Alloys and Compounds, 2009, 471, 222-240.	2.8	19
104	Hopkinson Bar Loaded Fracture Experimental Technique: A Critical Review of Dynamic Fracture Toughness Tests. Applied Mechanics Reviews, 2009, 62, .	4.5	141
105	Effect of Mo–Fe substitution on glass forming ability, thermal stability, and hardness of Fe–C–B–Mo–Cr–W bulk amorphous alloys. Materials Science & Engineering A: Structural Materials: Properties, Microstructure and Processing, 2008, 490, 221-228.	2.6	11
106	Preparation, characterization and mechanical performance of dense $\hat{I}^2$ -TCP ceramics with/without magnesium substitution. Journal of Materials Science: Materials in Medicine, 2008, 19, 3063-3070.	1.7	26
107	Aging and loading rate effects on the mechanical behavior of equine bone. Jom, 2008, 60, 39-44.	0.9	15
108	Devitrification and Cooling Rate Effects on Microstructure and Mechanical Properties in Fe <sub>57</sub> C <sub>9</sub> B <sub>11</sub> Mo <sub>12</sub> Cr <sub>8</sub> W <sub>3</sub> Bulk Metallic Glass. Advanced Engineering Materials, 2008, 10, 1056-1063.	1.6	3

#	Article	IF	CITATIONS
109	Development of quaternary Fe-based bulk metallic glasses. Materials Science & Engineering A: Structural Materials: Properties, Microstructure and Processing, 2008, 492, 230-235.	2.6	28
110	MECHANICAL AND MICROSTRUCTURAL PROPERTIES OF PTFEâ^•Alâ^•W SYSTEM. AIP Conference Proceedings, 2008, , .	0.3	6
111	Length and the Oxidation Kinetics of Chemical-Vapor-Deposition-Generated Multiwalled Carbon Nanotubes. Journal of Physical Chemistry C, 2008, 112, 10108-10113.	1.5	14
112	Effect of Mo–Fe substitution on glass forming ability and thermal stability of Fe–C–B–Mo–Cr–W bulk amorphous alloys. Journal of Non-Crystalline Solids, 2008, 354, 4550-4555.	1.5	5
113	Particle size effect on strength, failure, and shock behavior in polytetrafluoroethylene-Al-W granular composite materials. Journal of Applied Physics, 2008, 104, .	1.1	113
114	The influence of metallic particle size on the mechanical properties of polytetraflouroethylene-Al–W powder composites. Applied Physics Letters, 2008, 92, .	1.5	42
115	Optical determination of the flexural rigidity of carbon nanotube ensembles. Applied Physics Letters, 2008, 92, 173106.	1.5	8
116	The Mechanical Response of Aligned Carbon Nanotube Mats via Transmitted Laser Intensity Measurements. , 2008, , .		1
117	Experimental investigation of dynamic effects in a two-bar/three-point bend fracture test. Review of Scientific Instruments, 2007, 78, 063903.	0.6	32
118	Electroplating of Copper–Alumina Nanocomposite Films with an Impinging Jet Electrode. Journal of the Electrochemical Society, 2007, 154, D394.	1.3	16
119	Mechanical behavior of ultralong multiwalled carbon nanotube mats. Journal of Applied Physics, 2007, 101, 023512.	1.1	74
120	Modeling and validation of the large deformation inelastic response of amorphous polymers over a wide range of temperatures and strain rates. International Journal of Solids and Structures, 2007, 44, 7938-7954.	1.3	201
121	Conversion of sea urchin spines to Mg-substituted tricalcium phosphate for bone implants. Acta Biomaterialia, 2007, 3, 785-793.	4.1	63
122	Damage evolution in Ti6Al4V–Al3Ti metal-intermetallic laminate composites. Materials Science & Engineering A: Structural Materials: Properties, Microstructure and Processing, 2007, 443, 1-15.	2.6	57
123	Thermal history analysis of friction stir processed and submerged friction stir processed aluminum. Materials Science & Engineering A: Structural Materials: Properties, Microstructure and Processing, 2007, 465, 165-175.	2.6	53
124	Prediction of glass-forming compositions using liquidus temperature calculations. Materials Science & Engineering A: Structural Materials: Properties, Microstructure and Processing, 2007, 471, 135-143.	2.6	26
125	A microstructural investigation of adiabatic shear bands in an interstitial free steel. Materials Science & Engineering A: Structural Materials: Properties, Microstructure and Processing, 2007, 457, 205-218.	2.6	132
126	Hydrothermal synthesis of hydroxyapatite rods. Journal of Crystal Growth, 2007, 308, 133-140.	0.7	97

#	Article	IF	CITATIONS
127	Improved Pulse Shaping to Achieve Constant Strain Rate and Stress Equilibrium in Split-Hopkinson Pressure Bar Testing. Metallurgical and Materials Transactions A: Physical Metallurgy and Materials Science, 2007, 38, 2655-2665.	1.1	88
128	Dynamic Effects in Hopkinson Bar Four-Point Bend Fracture. Metallurgical and Materials Transactions A: Physical Metallurgy and Materials Science, 2007, 38, 2896-2906.	1.1	17
129	Fracture of Nitinol under Quasistatic and Dynamic Loading. Metallurgical and Materials Transactions A: Physical Metallurgy and Materials Science, 2007, 38, 2907-2915.	1.1	20
130	Superelasticity in a New BioImplant Material: Ni-rich 55NiTi Alloy. Experimental Mechanics, 2007, 47, 365-371.	1.1	68
131	Influence of Molecular Conformation on the Constitutive Response of Polyethylene: A Comparison of HDPE, UHMWPE, and PEX. Experimental Mechanics, 2007, 47, 381-393.	1.1	84
132	Conversion of bulk seashells to biocompatible hydroxyapatite for bone implants. Acta Biomaterialia, 2007, 3, 910-918.	4.1	197
133	Local Heating of Discrete Droplets Using Magnetic Porous Silicon-Based Photonic Crystals. Journal of the American Chemical Society, 2006, 128, 7938-7946.	6.6	61
134	Constitutive modeling of polymer materials at impact loading rates. European Physical Journal Special Topics, 2006, 134, 103-107.	0.2	2
135	Influence of temperature and strain rate on the mechanical behavior of three amorphous polymers: Characterization and modeling of the compressive yield stress. International Journal of Solids and Structures, 2006, 43, 2318-2335.	1.3	451
136	Prediction of carbon nanotube growth success by the analysis of carbon–catalyst binary phase diagrams. Carbon, 2006, 44, 267-275.	5.4	249
137	Response of NiTi shape memory alloy at high strain rate: A systematic investigation of temperature effects on tension–compression asymmetry. Acta Materialia, 2006, 54, 4609-4620.	3.8	106
138	Dynamic fracture of bovine bone. Materials Science and Engineering C, 2006, 26, 1325-1332.	3.8	100
139	Mechanical properties and structure of Strombus gigas, Tridacna gigas, and Haliotis rufescens sea shells: A comparative study. Materials Science and Engineering C, 2006, 26, 1380-1389.	3.8	129
140	Thermogravimetric Analysis of Synthesis Variation Effects on CVD Generated Multiwalled Carbon Nanotubes. Journal of Physical Chemistry B, 2006, 110, 1179-1186.	1.2	109
141	Creation of dense hydroxyapatite (synthetic bone) by hydrothermal conversion of seashells. Materials Science and Engineering C, 2006, 26, 1445-1450.	3.8	35
142	Synthesis optimization and characterization of multiwalled carbon nanotubes. Journal of Electronic Materials, 2006, 35, 211-223.	1.0	20
143	Carbon Nanotube-Based Fluid Flow/Shear Sensors. Materials Research Society Symposia Proceedings, 2006, 963, 1.	0.1	2
144	A unified model for stiffness modulus of amorphous polymers across transition temperatures and strain rates. Polymer, 2005, 46, 8194-8201.	1.8	149

#	Article	IF	CITATIONS
145	Submerged friction stir processing (SFSP): An improved method for creating ultra-fine-grained bulk materials. Materials Science & amp; Engineering A: Structural Materials: Properties, Microstructure and Processing, 2005, 402, 234-241.	2.6	153
146	Synthetic multifunctional metallic-intermetallic laminate composites. Jom, 2005, 57, 25-31.	0.9	146
147	Fracture of Ti-Al3Ti metal-intermetallic laminate composites: Effects of lamination on resistance-curve behavior. Metallurgical and Materials Transactions A: Physical Metallurgy and Materials Science, 2005, 36, 3217-3236.	1.1	65
148	Effects of ductile laminate thickness, volume fraction, and orientation on fatigue-crack propagation in Ti-Al3Ti metal-intermetallic laminate composites. Metallurgical and Materials Transactions A: Physical Metallurgy and Materials Science, 2005, 36, 1595-1608.	1.1	80
149	Response to the discussion by I.V. Rokach of the paper entitled: ?Analysis of the dynamic responses for a pre-cracked three-point bend specimen?. International Journal of Fracture, 2005, 131, 301-307.	1.1	2
150	Microstructure and exchange coupling in nanocrystalline Nd2(FeCo)14Bâ^•αâ€FeCo particles produced by spark erosion. Applied Physics Letters, 2005, 86, 122507.	1.5	10
151	Growth mechanism of vapor phase CVD-grown multi-walled carbon nanotubes. Carbon, 2005, 43, 2608-2617.	5.4	100
152	Growth of Well-Aligned Carbon Nanotube Structures in Successive Layers. Journal of Physical Chemistry B, 2005, 109, 12353-12357.	1.2	21
153	Analysis of modified split Hopkinson pressure bar dynamic fracture test using an inertia model. International Journal of Fracture, 2004, 126, 143-164.	1.1	12
154	Analysis of the dynamic responses for a pre-cracked three-point bend specimen. International Journal of Fracture, 2004, 127, 147-165.	1.1	41
155	Crack length calculation for bend specimens under static and dynamic loading. Engineering Fracture Mechanics, 2004, 71, 1971-1985.	2.0	30
156	Explosive welding of aluminum to aluminum: analysis, computations and experiments. International Journal of Impact Engineering, 2004, 30, 1333-1351.	2.4	136
157	Evaluation of dynamic fracture toughness KId by Hopkinson pressure bar loaded instrumented Charpy impact test. Engineering Fracture Mechanics, 2004, 71, 279-287.	2.0	56
158	Amorphous soft magnetic particles produced by spark erosion. Journal of Magnetism and Magnetic Materials, 2003, 254-255, 1-6.	1.0	42
159	Resistance-curve and fracture behavior of Ti–Al3Ti metallic–intermetallic laminate (MIL) composites. Acta Materialia, 2003, 51, 2933-2957.	3.8	212
160	Exchange-spring permanent magnet particles produced by spark-erosion. Applied Physics Letters, 2003, 82, 1574-1576.	1.5	14
161	SYNTHETIC MULTI-FUNCTIONAL MATERIALS BY DESIGN USING METALLIC-INTERMETALLIC LAMINATE (MIL) COMPOSITES. , 2003, , 243-254.		3
162	Dislocation microstructure and internal-stress measurements by convergent-beam electron diffraction on creep-deformed Cu and Al. Metallurgical and Materials Transactions A: Physical Metallurgy and Materials Science, 2002, 33, 311-317.	1.1	24

#	Article	IF	CITATIONS
163	The variation of dislocation density as a function of the stacking fault energy in shock-deformed FCC materials. Materials Science & Engineering A: Structural Materials: Properties, Microstructure and Processing, 2002, 328, 256-266.	2.6	64
164	Thick amorphous ferromagnetic coatings via thermal spraying of spark-eroded powder. Materials Letters, 2001, 48, 184-187.	1.3	20
165	The influence of stacking fault energy on the mechanical behavior of Cu and Cu-Al alloys: Deformation twinning, work hardening, and dynamic recovery. Metallurgical and Materials Transactions A: Physical Metallurgy and Materials Science, 2001, 32, 135-145.	1.1	395
166	Microstructure evolution in metal-intermetallic laminate (MIL) composites synthesized by reactive foil sintering in air. Metallurgical and Materials Transactions A: Physical Metallurgy and Materials Science, 2001, 32, 1493-1505.	1.1	164
167	A metallographic and quantitative analysis of the influence of stacking fault energy on shock-hardening in Cu and Cu–Al alloys. Acta Materialia, 2001, 49, 427-438.	3.8	91
168	Microstructural evolution in adiabatic shear bands in Ta and Ta–W alloys. Acta Materialia, 2001, 49, 2905-2917.	3.8	167
169	Determination of internal stresses in cyclically deformed copper single crystals using convergent-beam electron diffraction and dislocation dipole separation measurements. Acta Materialia, 2000, 48, 4247-4254.	3.8	49
170	Quasi-static and dynamic mechanical response of Haliotis rufescens (abalone) shells. Acta Materialia, 2000, 48, 2383-2398.	3.8	337
171	Modeling solid-particle erosion of ductile alloys. Metallurgical and Materials Transactions A: Physical Metallurgy and Materials Science, 1999, 30, 1763-1774.	1.1	64
172	Influence of grain size on the constitutive response and substructure evolution of MONEL 400. Metallurgical and Materials Transactions A: Physical Metallurgy and Materials Science, 1999, 30, 1235-1247.	1.1	64
173	Simultaneous oxidation and sigma-phase formation in a stainless steel. Metallurgical and Materials Transactions A: Physical Metallurgy and Materials Science, 1999, 30, 355-362.	1.1	25
174	A model for microstructure evolution in adiabatic shear bands. Metallurgical and Materials Transactions A: Physical Metallurgy and Materials Science, 1998, 29, 191-203.	1.1	128
175	Modeling the strain-rate dependence of fatigue life of hot-pressed silicon nitride. Mechanics of Materials, 1998, 29, 253-273.	1.7	2
176	Behavior of Nicalonâ,"¢-fiber-reinforced glass-matrix composites under thermal cycling conditions. Composites Part A: Applied Science and Manufacturing, 1998, 29, 1343-1352.	3.8	27
177	Effect of Grainâ€Boundary Phase on Dynamic Compression Fatigue in Hotâ€Pressed Silicon Nitride. Journal of the American Ceramic Society, 1998, 81, 129-139.	1.9	13
178	Modeling the mechanical behavior of tantalum. Metallurgical and Materials Transactions A: Physical Metallurgy and Materials Science, 1997, 28, 113-122.	1.1	30
179	Recrystallization kinetics within adiabatic shear bands. Acta Materialia, 1997, 45, 635-649.	3.8	203
180	Bauschinger effect in haynes 230 alloy: Influence of strain rate and temperature. Metallurgical and Materials Transactions A: Physical Metallurgy and Materials Science, 1996, 27, 1739-1748.	1.1	13

#	Article	IF	CITATIONS
181	Dynamic Bauschinger effect. Acta Materialia, 1996, 44, 2797-2807.	3.8	24
182	On the structure of faults in pyrites. Philosophical Magazine A: Physics of Condensed Matter, Structure, Defects and Mechanical Properties, 1996, 73, 779-801.	0.8	0
183	Deformation behavior and failure mechanisms in particulate reinforced 6061 Al metal-matrix composites. Materials Science & amp; Engineering A: Structural Materials: Properties, Microstructure and Processing, 1995, 202, 63-75.	2.6	30
184	Influence of subsolvus thermomechanical processing on the low-cycle fatigue properties of haynes 230 alloy. Metallurgical and Materials Transactions A: Physical Metallurgy and Materials Science, 1995, 26, 673-689.	1.1	13
185	Shock-loading response of 6061- T6 aluminum metal-matrix composites. Metallurgical and Materials Transactions A: Physical Metallurgy and Materials Science, 1995, 26, 2545-2553.	1.1	3
186	Influence of peak pressure and temperature on the structure/property response of shock- loaded Ta and Ta-10W. Metallurgical and Materials Transactions A: Physical Metallurgy and Materials Science, 1995, 26, 2555-2563.	1.1	94
187	On the nature of faults in MoSi2. Philosophical Magazine A: Physics of Condensed Matter, Structure, Defects and Mechanical Properties, 1995, 72, 1-19.	0.8	11
188	Electron microscopy of shock-synthesized silicides and aluminides. AIP Conference Proceedings, 1994, ,	0.3	0
189	Effects of shock loading on a solid-solution strengthened superalloy. AIP Conference Proceedings, 1994, , .	0.3	Ο
190	Quenching and thermal cycling effects in a 1060-Al matrix-10vol.%Al2O3 particulate reinforced metal matrix composite. Materials Science & Engineering A: Structural Materials: Properties, Microstructure and Processing, 1993, 171, 181-189.	2.6	9
191	Defect Structures and Planar Faults in Plasma Spray Deposited MoSi2. Materials Research Society Symposia Proceedings, 1992, 288, 1123.	0.1	2
192	SHOCK SYNTHESIS OF SILICIDES. , 1992, , 629-632.		2
193	Microstructural characterization of self-propagating high-temperature synthesis/ dynamically compacted and hot-pressed titanium carbides. Metallurgical and Materials Transactions A - Physical Metallurgy and Materials Science, 1992, 23, 87-97.	1.4	34
194	Transmission electron microscope in situ fatigue experiments: A computer-control approach. Journal of Electron Microscopy Technique, 1991, 17, 351-355.	1.1	1
195	In-situ observations of microvoid coalescence: Stacking fault energy effects. Proceedings Annual Meeting Electron Microscopy Society of America, 1990, 48, 520-521.	0.0	Ο
196	The influence of stacking fault energy on ductile fracture micromorphology. Journal of Materials Science, 1988, 23, 2220-2224.	1.7	9
197	The apparent 'five-fold' nature of large T2 (Al6Li3Cu) crystals. Metallurgical and Materials Transactions A - Physical Metallurgy and Materials Science, 1988, 19, 2875-2884.	1.4	19
198	Convergent beam electron diffraction analysis of theT 1 (Al2CuLi) phase in Al-Li-Cu alloys. Metallurgical and Materials Transactions A - Physical Metallurgy and Materials Science, 1988, 19, 2885-2891.	1.4	25

#	Article	IF	CITATIONS
199	A non-icosahedral T <sub>2</sub> (Al <sub>6</sub> Li <sub>3</sub> Cu) phase. The Philosophical Magazine: Physics of Condensed Matter B, Statistical Mechanics, Electronic, Optical and Magnetic Properties, 1988, 57, 535-546.	0.6	24
200	Experimental conditions affecting coherent bremsstrahlung in Xâ€ray microanalysis. Journal of Microscopy, 1987, 147, 15-35.	0.8	10